Journal of Polymer Science Part A: Polymer Chemistry Journal

Copy of e-mail Notification

Journal of Polymer Science Part A: Polymer Chemistry Published by John Wiley & Sons, Inc.

Dear Author,

Your article is ready for your final content correction within our rapid production workflow. The PDF file found at the URL given below is generated to provide you with a proof of the content of your manuscript. Once you have submitted your corrections, the production office will finalize the layout of your article for publication.

Any corrections should be returned to jrnlprodpola@cadmus.com within 2 business days after receipt of this email in order to achieve our goal of publishing your article online 15 days from the day final data was received.

http://115.111.50.156/jw/retrieval.aspx?pwd=9b089c07ac44

Login: your e-mail address
Password: 9b089c07ac44

Making corrections

In order to speed the proofing process, we strongly encourage authors to correct proofs by annotating PDF files. Instructions on the Annotation of PDF files can be found on the journal homepage in the Author Guidelines:

http://onlinelibrary.wiley.com/journal/10.1002/(ISSN)1099-0518/homepage/ForAuthors.html

Technical Problems

If you experience technical problems, please contact Balaji/Sam at wileycs@kwglobal.com

Contact

Return your corrections (always cite article number, JPOL-A-14-0425.R1) to: jrnlprodpola@cadmus.com
Questions can be directed to the Production Editor, POLA at:
E-mail: jrnlprodpola@cadmus.com

Please refer to the journal acronym and always cite the article number

Journal of Polymer Science, Part A: Polymer Chemistry

Polymer Chemistry

Production Editor, POLA
E-mail: jrnlprodpola@cadmus.com

Please refer to the journal acronym and article number in all correspondence.

Dear Author,

Please correct your galley proofs carefully and return within 2 business days to jrnlprodpola@cadmus.com.

This will be your only chance to review these proofs. Please note that the volume and page numbers shown on the proofs are for position only.

The editors reserve the right to publish your article without your corrections if they are not received in time. Note that the author is liable for damages arising from incorrect statements, including misprints.

Please limit corrections to errors already in the text; cost incurred for any further changes or additions will be charged to the author, unless such changes have been agreed upon by the editor.

Please annotate all corrections on the supplied PDF. Instructions can be found on the journal homepage.

To avoid commonly occurring errors, please ensure that the following important items are correct in your proofs (please note that once your article published online, no further corrections can be made):

- ☐ Names of all authors present and spelled correctly
- ☐ Addresses and postcodes correct
- ☐ E-mail address of corresponding author correct and current
- ☐ Title of article correct
- ☐ All figures included and in the correct order
- ☐ All tables and equations correct (symbols and superscripts)
- ☐ All queries (included on the last page) answered

Note: the resolution of the figures in the PDF proofs is intentionally of lower quality to facilitate internet delivery. These images will appear at higher resolution and sharpness in the printed article.

Reprint Purchases: Should you wish to purchase additional copies of your article, please click on the link and follow instructions provided:
https://caesar.sheridan.com/reprints/redir.php?pub=10089&acro=POLA

J_ID: z8g Customer A_ID: POLA27375 Cadmus Art: POLA27375 Ed. Ref. No.: 14-0425.R1 Date: 28-August-14 Stage: Page: 1

Different Synthetic Pathways of Nanoparticle-Cored Dendrimers (NCDs): Effects on the Properties and their Application as Redox Active Centers

Julieta I. Paez,[1]* Pablo Froimowicz,[2]† Katharina Landfester,[2] Verónica Brunetti,[3] Miriam Strumia[1]

[1]IMBIV-CONICET, Departamento de Química Orgánica, Facultad de Ciencias Químicas, Universidad Nacional de Córdoba, Haya de la Torre y Medina Allende, Ciudad Universitaria (X5000HUA), Córdoba, Argentina
[2]Max Planck Institute for Polymer Research, Ackermannweg 10, 55128, Mainz, Germany
[3]INFIQC-CONICET, Departamento de Fisicoquímica, Facultad de Ciencias Químicas, Universidad Nacional de Córdoba, Haya de la Torre y Medina Allende, Ciudad Universitaria (X5000HUA), Córdoba, Argentina
Correspondence to: M. C. Strumia (E-mail: mcs@fcq.unc.edu.ar or paez@mpip-mainz.mpg.de)

Received 3 June 2014; accepted 13 August 2014; published online 00 Month 2014
DOI: 10.1002/pola.27375

ABSTRACT: The synthesis of nanoparticle-cored dendrimers (NCDs) through surface functionalization of iron oxide nanoparticles (γ-Fe_2O_3) by combining the conventional silane coupling agent 3-(aminopropyl) triethoxysilane (APS) with dendritic moieties is studied and presented. Much emphasis has been put on the role played by each modifier and how they interact not only between themselves, but also with the dispersing media wherein the resulting NCDs are. As a part of the functionalization, redox-active nitro groups were introduced onto the surface of each synthesized NCD thus making them electrochemically active. Then, the obtained NCDs were immobilized onto glassy carbon electrodes. Both the NCDs and modified electrodes are expected to be eventually exploited in analytical and sensing applications. © 2014 Wiley Periodicals, Inc. J. Polym. Sci., Part A: Polym. Chem. **2014**, *00*, 000–000

KEYWORDS: dendronization; immobilization; nanoparticle-cored dendrimers; redox-active surfaces; surface functionalized nanoparticles

AQ1

INTRODUCTION Tailored synthesis of hybrid nanoparticles (NPs) presenting well-defined functionalities is currently of crucial relevance in materials science since the resulting nanohybrids find an extensive scope of application, such as in medicine,[1,2] catalysis,[3] films and coatings,[4] as well as in analytical[5] and sensing purposes.[6,7] For all nanohybrids to be applicable specific features must be considered, such as dispersibility, stability, and reactivity. The manner in which these parameters interact between themselves and with the surrounding dispersing media must also be taken into consideration.[8] Understandably, most of these features and interactions strongly depend on the chemical composition of the NPs' surface. Organic and macromolecular chemistries offer efficient methodologies to carry out those controlled functionalizations on different kind of NPs' surfaces including inorganic ones,[9] thus forming straightforward applicable organic–inorganic hybrid nanomaterials. Thus, ligand exchange, chemical functionalization with small organic molecules, dendritic and linear (co-)polymers, as well as layer-by-layer deposition and monomer polymerization are some examples of those strategies to enhance—among others—the NPs' reactivity, stability, and dispersibility.[10] Moreover, these surface functionalizations allow for the simultaneous incorporation of different functional groups, which may be exploited afterward for further physical/chemical functionalization of the NPs toward specific applications.[11–15]

In the present contribution, we focused on the organic surface modification of inorganic NPs (γ-Fe_2O_3) combining different strategies, the evaluation on how each modifier acts and interacts with the other modifiers and with the medium in which the final product is, along with the subsequent study of applicability of the resulting nanohybrids toward the generation of electrochemical sensors. To obtain the nanohybrids, a combination of organic functionalizations consisting in silanization and dendronization was carried out. While silanization was mainly performed to introduce architectural differences in the organic content, dendronization was carried out to introduce the electroactive $-NO_2$ groups.

*Present address: Max Planck Institute for Polymer Research, Ackermannweg, 10, 55128, Mainz, Germany

†Present address: Pagora—Grenoble Institute of Technology, 461, rue de la Papeterie, St-Martin-d'Hères Cedex, 38402, France

ID: thangaraj.n Time: 20:51 I Path: N:/3b2/POLA/Vol00000/140260/APPFile/JW-POLA140260

J_ID: z8g Customer A_ID: POLA27375 Cadmus Art: POLA27375 Ed. Ref. No.: 14-0425.R1 Date: 28-August-14 Stage: Page: 2

Nanoparticle-cored dendrimers (NCDs) are highly defined, controlled core-shell nanocomposites formed by an inorganic nanoparticle (the core) positioned at the center of the structure and an organic shell given by dendrons attached to the core in a radial way by specific interactions. When a certain density of dendritic wedges is attained, NCD structure is comparable to a dendrimer backbone since both feature defined and differentiable exterior, interior and void spaces (cavities). Moreover, the number and nature of the outermost functional groups determine the characteristic properties of these hybrid materials, like solubility, reactivity or permeability through the dendritic barrier.[16–19]

Different strategies to prepare NCDs have been described.[16,18] The introduction of dendritic moieties on NPs can be performed following different strategies: direct dendron binding to the NP surface,[20,21] via ligand exchange of previously stabilized NPs,[22,23] through dendronization[24] or via divergent dendritic growing[25] from functionalized NPs. NCDs synthesized in diverse ways may vary in their structural parameters such as dendron loading, presence of other organic molecules within the modifying layer, ordering and packing density of the coating. Those differences could easily affect macroscopic and physicochemical properties.

Therefore, different NCDs bearing aromatic dendrons and terminal nitro groups in their periphery, able to assemble onto carbon surfaces were synthesized following three different pathways and fully characterized. The prepared NCDs were then immobilized on glassy carbon (GC) electrodes in order to generate electroactive surfaces. The aromatic rings were expected to act as carbon-anchorage sites providing stable attachment of the NCDs on the surfaces, whereas the nitro-end groups provide redox-active moieties on the nanostructured electrode able to be exploited electrochemically for sensing purposes.[26,27] The NCDs were synthesized following three different pathways, the first by direct dendronization of the NPs; the second by modifying first the NPs' surface with a silane coupling agent and then dendronizing them; and the third by modifying with the same silane coupling agent those NPs that were directly dendronized at first. One important structural feature studied for the synthesized NCDs was how the different roles of the silane coupling agent affect the general properties of the resulting products. Finally, the applicability of the synthesized NPs was studied toward the preparation of modified GC electrodes.

EXPERIMENTAL

Materials and Equipment

Dendron ((3,5-*Bis*(3,5-dinitrobenzoylamino) benzoyl chloride) (G1-$ClNO_2$) was synthesized following a procedure previously reported by our group[28] from its Kakimoto's type precursor (3,5-*Bis*(3,5-dinitrobenzoylamino) benzoic acid (G1-NO_2);[29] 3-(aminopropyl) triethoxysilane (APS, Sigma Aldrich, 99%) was used as received; *N,N*-dimethyl acetamide (DMAc, Tedia) and toluene (Ciccarelli) were dried and stored over 4 Å molecular sieves. Acetonitrile (ACN, Sintorgan) and dimethyl sulfoxide (DMSO, Sintorgan) were HPLC grade and used as received. Iron oxide maghemite (γ-Fe_2O_3) nanoparticles (NPs, Integran Tech. Inc.), with a nominal size of 9 nm, were used as received. The rest of commercially available chemicals were reagent grade and used without further purification. All solutions were prepared immediately prior to use. Phosphate buffer solutions (PBS, 0.1 M Na_2HPO_4/NaH_2PO_4) were prepared. Water was purified with a Millipore Milli-Q system. APS coupling reactions were performed in a TestLab ultrasound bath at 30 °C. Dialyses were carried out using benzoylated cellulose membranes, 32 mm wide (Sigma-Aldrich), MWCO = 2000 g mol^{-1}, at constant stirring. Centrifugation was performed in a Christ centrifuge at 6000 *g*.

Conventional transmittance (FT-IR) and diffuse reflection Fourier transform (DRIFT) infrared spectra were recorded using a Nicolet-5SXC spectrometer, 64 scans in average, at a resolution of 4 cm^{-1}. Infrared data were processed using the EZ Omnic E.S.P. 5.1 software. The spectra shown are normalized. The physical mixtures between NPs and dendron (**PM 1**) as well as NPs-APS and dendron (**PM 2**) were prepared using the same molar amount of dendron used for the covalent binding reactions (see synthesis of NCD-1 and NCD-2, respectively). UV spectra were recorded using a Shimadzu MultiSpect 1501 spectrometer, between 200 and 800 nm at 25 °C. TGA measurements were performed using a H1-Res M TGA 2950 from TA Instruments, under nitrogen flux (50 mL min^{-1}), in sealed aluminum pans, heating up to 1100 °C at 10 °C min^{-1}. The equipment was calibrated through the determination of the Curie point. Organic contents were calculated following a reported procedure.[30] TEM images were recorded using a Philips CM12 (FEI, OR) electronic microscope operated at 100 kV. Samples were prepared by drop-casting the proper dispersion onto standard carbon-coated colodion films copper grids (200-mesh), followed by the natural solvent evaporation. For each sample, a minimum of four different regions were studied. The images were analyzed using the ImageJ 1.32j software.

Chemical Modification of γ-Fe_2O_3 Nanoparticles

Synthesis of NCD-1 (Route 1)

In a three-neck flask equipped with a magnetic stirrer and a nitrogen inlet, dendron G1-$ClNO_2$ (5.3×10^{-5} mol) was synthesized.[28] After cooling the flask at −5 °C, a dispersion of NPs (100 mg, 5.3×10^{-5} mol -OH) in DMAc (10 mL) was added. The system was stirred (1500 rpm) at −5 °C for 6 h, then allowed to reach room temperature and stirred for additional 18 h. A dark red dispersion was obtained, which was poured into cold $HCl_{(aq)}$ (1.5 M, 50 mL) to hydrolyze the remaining G1-$ClNO_2$ and then centrifuged to separate the particles. The solid was washed and recovered through exhaustive redispersion-centrifugation cycles in water. The obtained product was dialyzed against acetone to eliminate the non-covalently attached dendron, followed by two washing and centrifugation cycles in acetone. The completion of every purification step was determined by means of FT-IR, checking the absence of impurities in the supernatant. The product was dried under vacuum at 45 °C until constant

ID: thangaraj.n Time: 20:51 I Path: N:/3b2/POLA/Vol00000/140260/APPFile/JW-POLA140260

J_ID: z8g Customer A_ID: POLA27375 Cadmus Art: POLA27375 Ed. Ref. No.: 14-0425.R1 Date: 28-August-14 Stage: Page: 3

weight (~48 h), obtaining a reddish-brown solid (50 mg). Yield (in mass) = 50%. DRIFT ν_{max} (cm^{-1}) = 3400 (OH str), 3101 (CH str), 2958–2026 (CH str), 1700–1610 (C=O ester str and amide Bands I-II), 1540 and 1344 (nitro asymmetric and symmetric str); 640–560 (Fe-O str). Organic content (by TGA): 5%.

Synthesis of NPs-APS (Route 2, First Step)

The silanization of NPs with APS was achieved following a modified procedure based on previous reports.[31,32] In a two-neck flask equipped with a nitrogen inlet, a dispersion of NPs (500 mg, 2.6×10^{-4} mol -OH) in toluene (100 mL) was prepared. After adding APS (1 mL, 4.34×10^{-3} mol) via syringe, the mixture was sonicated for 3 h at 30 °C and then centrifuged. The modified NPs were washed and recovered by redispersion-centrifugation cycles in THF to eliminate the non-attached APS. The absence of impurities in the supernatant was verified by FT-IR. The precipitate was dried under vacuum at 45 °C until constant weight (~48 h), obtaining a reddish-brown solid (280 mg). Yield (in mass) = 56%. DRIFT ν_{max} (cm^{-1}) = 3440 (OH str), 2940-2876 (aliphatic CH str); 1560 (NH bend); 1130–1030 (Si-O-Si and Fe-O-Si str); 640–560 (Fe-O str). Organic content (by TGA): 4%.

Synthesis of NCD-2 (Route 2, Second Step)

In a three-neck flask equipped with a magnetic stirrer and a nitrogen inlet, G1-$ClNO_2$ (5.3×10^{-5} mol) was synthesized.[28] After cooling the flask at −5 °C, a dispersion of NPs-APS (100 mg, 5.3×10^{-5} mol -OH) in DMAc (10 mL) was added. The system was stirred (1500 rpm) at −5 °C for 6 h, then allowed to reach room temperature and stirred for additional 18 h. A dark red dispersion was obtained, which was poured into cold $HCl_{(aq)}$ (1.5 M, 50 mL) and centrifuged. The solid was washed and separated through exhaustive redispersion-centrifugation cycles in water and acetone to eliminate the non-covalently attached dendron. The absence of impurities in the supernatant was determined by means of FT-IR. The product was dried in vacuum at 45 °C until constant weight (~48 h), obtaining a reddish-brown solid (35 mg). Yield (in mass) = 35%. DRIFT ν_{max} (cm^{-1}) = 3440 (OH str), 2960–2853 (CH str); 1680–1600 (amide bands I-II); 1541 and 1345 (nitro, asymmetric and symmetric str); 1130–1030 (Si-O-Si and Fe-O-Si str); 640–560 (Fe-O str). Organic content (by TGA): 6%.

Synthesis of NCD-3 (Route 3)

In a two-neck flask equipped with a nitrogen inlet, a dispersion of NCD-1 (24.8 mg) in toluene (5 mL) was prepared. After adding APS (0.05 mL, 0.212 mmol) via syringe, the mixture was sonicated for 3 h at 30 °C and then centrifuged. The modified NPs were washed and recovered by redispersion-centrifugation cycles in THF to remove all unattached APS. The absence of impurities in the supernatant was verified by FT-IR. The precipitate was dried under vacuum at 45 °C until constant weight (~48 h), obtaining a reddish-brown solid (20 mg). Yield (in mass) = 81%. DRIFT ν_{max} (cm^{-1}) = 3420 (OH str); 2970–2880 (CH str); 1650–1560 (C=O ester str and NH bend); 1543 and 1345 (nitro, asymmetric and symmetric str); 1130–1000 (Si-O-Si and Fe-O-Si str); 640-560 (Fe-O str). Organic content (by TGA): 10%.

Dispersibility and Stability Studies

G1-NO_2, APS, the unmodified and all modified NPs dispersions were characterized by UV-Vis spectroscopy in several organic solvents such as toluene, acetone, ACN, DMF, and DMSO. All UV-Vis spectroscopy studies were carried out using ACN as solvent due to its low cut-off wavelength (ca. 190 nm). To this end, dendron solutions of different concentrations (from 1.8 to 15.0 mM), APS solutions (17.0 mM), and dispersions of unmodified and modified NPs (from 0.100 to 0.005 mg mL^{-1}) were prepared. All dispersions were sonicated for 5 min at 25 °C, rapidly transferred to a cuvette and immediately measured. Spectra were recorded every 3 min for a total time of 12 min. Dispersibility was evaluated qualitatively. The absorbance values at 400 nm were used to calculate dispersion stability as the decay of absorption as a function of time at the mentioned wavelength after 12 min as follows: Abs. decay = $100\ (Abs_{t=0} - Abs_{t=12})/Abs_{t=0}$.

Electrochemical Measurements

Electrochemical measurements were performed using an Autolab electrochemical analyzer and a conventional three-electrode system, comprising a glassy carbon working electrode, a platinum foil as counter-electrode, and an Ag/AgCl 3.0 M NaCl electrode (from BAS) as reference. All potentials were reported *versus* the Ag/AgCl reference electrode at room temperature. Nitrogen gas was used to deaerate all aqueous solutions before use.

Preparation of the Working Electrode

3.0 mm-GC electrodes (CH Instruments, Inc. Austin, TX) were polished with 1.0, 0.3, and 0.05 mm alumina slurry on a microcloth pad, rinsed with water and ethanol, sonicated for 10 min in distilled water and dried under nitrogen flux.

Attachment of Unmodified and Modified NPs onto GC by Self-Assembly

A cleaned GC electrode was incubated in a dispersion of the corresponding NCD (1 mg mL^{-1}) in DMSO at intervals ranging from 15 min up to overnight. The modified surface was subsequently rinsed with copious volumes of DMSO, water and ethanol, and measured immediately by cyclic voltammetry (CV).

The following control experiments were carried out: first, a cleaned GC surface was drop-casted with a dispersion of unmodified NPs (1 mg mL^{-1}) in DMSO, and it was naturally evaporated. Then, the modified electrode was measured by means of CV. A second control experiment similar in procedure was performed but using NPs-APS (1 mg mL^{-1}) dispersed in DMSO.

RESULTS AND DISCUSSION

Experimental Design and Synthesis

The syntheses of the NCDs were carried out by covalent attachment of a first-generation dendron (G1-NO_2) onto γ-

ID: thangaraj.n Time: 20:51 I Path: N:/3b2/POLA/Vol00000/140260/APPFile/JW-POLA140260

J_ID: z8g Customer A_ID: POLA27375 Cadmus Art: POLA27375 Ed. Ref. No.: 14-0425.R1 Date: 28-August-14 Stage: Page: 4

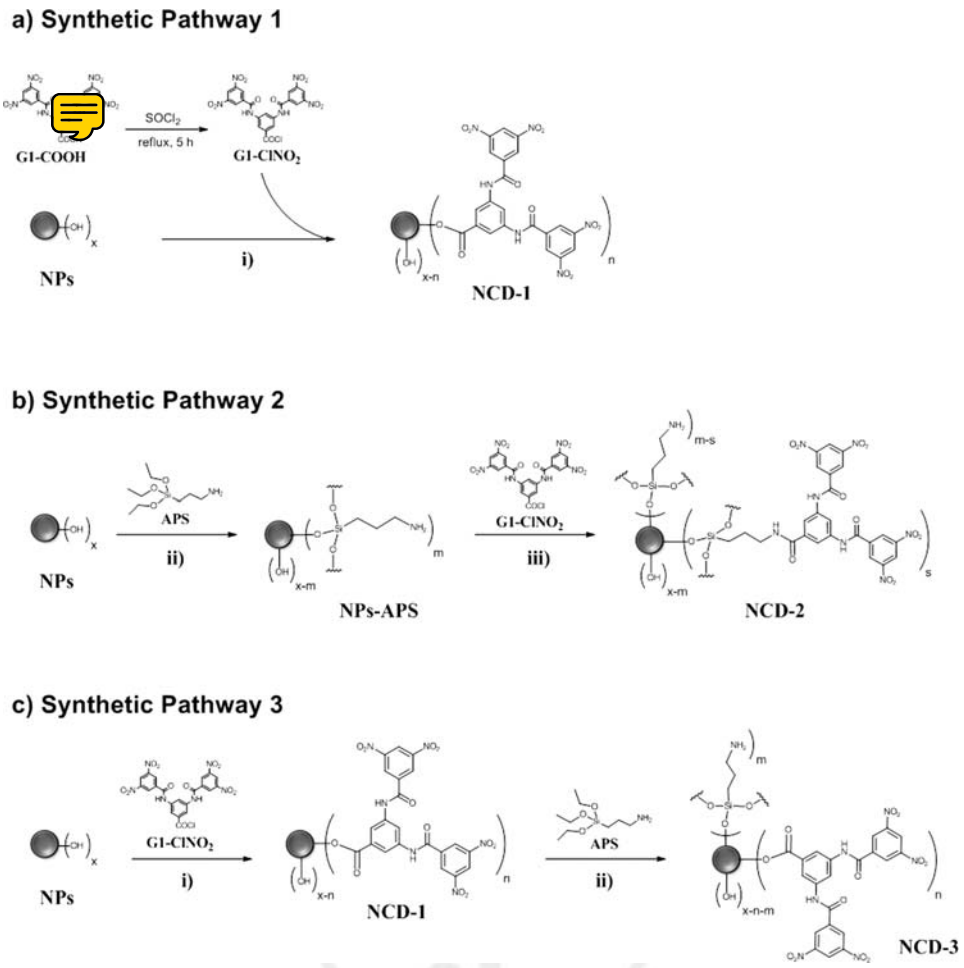

SCHEME 1 Synthetic pathways followed to prepare NCDs containing aromatic nitro-end groups: (a) Pathway 1: dendron is directly attached to the NPs via dendronization; (b) Pathway 2: achieved in two steps, once silanization with APS is finished, dendronization is carried out, placing APS between the rigid dendron and the hard NPs' surface acting as a flexible linker; (c) Pathway 3: in this case **NCD-1** is used as starting material for coupling the APS agent, introducing a silane layer as a synthetic complement to the already incorporated dendron. Reaction conditions: (i and iii) **G1-ClNO$_2$,** DMAc, 0 °C—r.t., N_2, 24 h; (ii and iv) APS, toluene, ultrasonic bath, N_2, 30 °C, 3 h.

Fe_2O_3 NPs following three different pathways as presented in Scheme 1.

The first pathway involved first the activation of the dendron by forming its acid chloride,[33] which is then reacted with the NPs, thus binding the dendron directly onto NPs [see Pathway 1, Scheme 1(a)]. After rigorous and spectroscopically controlled purification steps, **NCD-1** was obtained as a reddish-brown powder (50%).

The second synthetic pathway was a modified procedure from previously reported ones[24,34] consisting in modifying first the NPs with 3-(aminopropyl) triethoxysilane (APS), and making the dendronization as a second step. Thus, NPs were silanized and purified generating **NPs-APS** as a reddish-brown powder (56%). Then, **NCD-2** was obtained by dendronizing the freshly synthesized precursor **NPs-APS** as a reddish-brown powder (35%). The procedure is shown in Scheme 1(b) as Pathway 2. A consequence of this method is that APS, or a layer formed by polymerized APS, could be viewed as a flexible linker or spacer between the rigid dendron and the hard NPs' surface.

Finally, the third followed pathway exploited the freshly generated **NCD-1** as starting material to be reacted with APS, thus obtaining **NCD-3** as a reddish-brown solid (81%). This method is shown as Pathway 3 in Scheme 1(c). Unlike the synthesis of **NCD-2**, silanization to generate **NCD-3** takes place only after the dendron is already attached to the hard NPs' surface. Therefore, APS plays a different role in **NCD-3** than in **NCD-2**, being in this case considered a synthetic complement in this new structure.

Clearly, these three strategies lead to three different NCDs with unlike nanostructured and chemical compositions on their surfaces, which may therefore present different features. To gain deeper insights on these systems all syntheses were performed in a comparative fashion, meaning that

ID: thangaraj.n Time: 20:51 I Path: N:/3b2/POLA/Vol00000/140260/APPFile/JW-POLA140260

J_ID: z8g Customer A_ID: POLA27375 Cadmus Art: POLA27375 Ed. Ref. No.: 14-0425.R1 Date: 28-August-14 Stage: Page: 5

those steps involving G1-$ClNO_2$ binding were performed using equal molar amounts of dendron, and those where APS was incorporated were also performed using equal molar amounts of the silane agent.

Synthesis of NCDs Bearing Terminal Nitro Groups

All intermediates and final products were fully characterized by TGA, TEM, and UV-Vis and IR spectroscopy. The DRIFT method was used since it has been previously shown to be a powerful technique to gain better insight into the chemical composition at the surface and/or the outer part of NPs.[35–37]

DRIFT Characterization

NCD-1

F1 Figure 1(a–d) shows the DRIFT spectra of the unmodified NPs, the pure dendron (its chemical structure is shown in Scheme 1, Synthetic Pathway 1), a physical mixture formed by the unmodified NPs and the dendron (**PM 1**), and **NCD-1**. The latter evidences new signals attributed to the incorporation of dendron: C-H stretching (3101, 2958, and 2926 cm^{-1}), ester C=O stretching and amide bands I-II (wide band at 1700–1610 cm^{-1}); nitro asymmetric and symmetric stretchings (1540 and 1344 cm^{-1}, respectively), and out-of-plane aromatic C-H bending (910 cm^{-1}). Other characteristic signals from γ-Fe_2O_3 such as O-H stretching (3400 cm^{-1}) and Fe-O stretching (640–560 cm^{-1}) are also observed. In fact, the strong intensity of the former indicates a high amount of remaining non-reacted hydroxyl groups, suggesting a low dendron loading.

Note that the spectrum of **NCD-1** [Fig. 1(d)] shows three C-H stretching bands. Although with a decreased intensity, the first one is located at the very same wavenumber that the aromatic C-H stretching of the pure dendron (3101 cm^{-1}), whereas the other two bands (2958 and 2926 cm^{-1}) are located at lower wavenumbers than those of normal aromatic C-H stretching (>3000 cm^{-1}). The presence of aliphatic impurities or unattached dendron in the sample is discarded since the product was thoroughly purified; these new bands may indeed belong to aromatic C-H groups vibrating at lower frequencies due to the covalent binding of the dendron onto the NPs.

A control experiment to determine whether this effect (shifting to lower wavenumbers on the spectrum) actually takes place or is an artifact was performed. To this end, a physical mixture between unmodified NPs and dendron (**PM 1**) was prepared and studied. Spectrum c (**PM 1**) shows to be the net sum of the spectra of the two components (NPs and dendron). Moreover, it clearly evidences the presence of the aromatic C-H stretching band at 3101 cm^{-1} as for the pure dendron (b) and no bands at ~2900 cm^{-1}. Thus, such new bands (2958 and 2926 cm^{-1}) in **NCD-1** spectrum may be assigned to aromatic C-H stretching whose frequency has lowered as a consequence of the covalent attachment of the dendron onto the NPs' surface. Previous reports on the covalent binding of aliphatic molecules onto plane and curved metallic surfaces via self-assembly have shown a similar

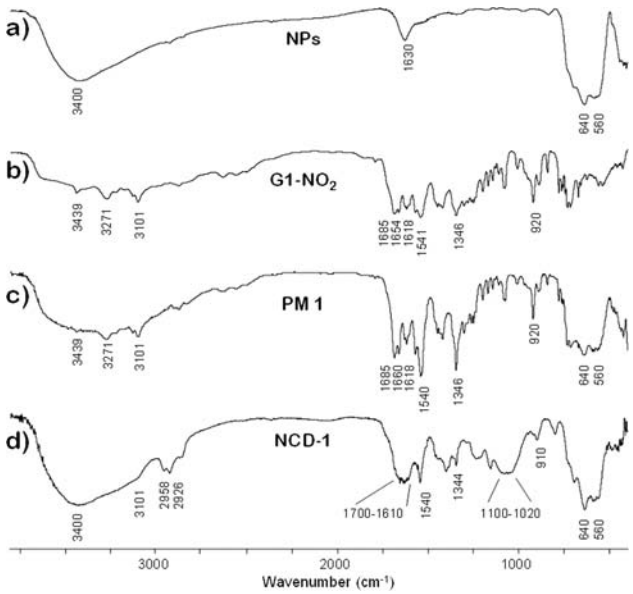

FIGURE 1 DRIFT spectra of the unmodified NPs (a); pure **G1-NO_2** (b); **PM 1**, the physical mixture between NPs + **G1-NO_2** (c); and **NCD-1** (d).

effect.[38,39] These molecules may experience conformational changes related to their order and packing onto the surface. This process affects their C-H stretching vibrations either varying their intensity and/or lowering their frequencies in relation to the pure compound.[38,39] Whereas this effect is well-documented for aliphatic molecules, to the best of our knowledge this is not the case for the covalent binding of aromatic molecules on surfaces. However, a recent work by Griffete et al.[40] on the covalent functionalization of magnetite NPs with aromatic molecules through diazonium salt coupling evidences a similar effect as in our case, where the aromatic C-H vibrations have shifted to lower frequencies in relation to the pure compound; unfortunately, the authors did not discuss this change any further.

Another important feature in the **NCD-1** spectrum is the out-of-plane aromatic bending of the dendron. This peak present at 920 cm^{-1} in both spectra the pure compound and the PM 1 respectively also shows a small frequency lowering to 910 cm^{-1} in the **NCD-1** spectrum. This effect may have the same origin as the one previously shown for the C-H stretching vibrations. Finally, the presence of the two wide bands located between 1700 and 1610 cm^{-1} (ester C=O stretching) and between 1100 and 1020 cm^{-1} (combination of ester C-O stretching bands) in the **NCD-1** spectrum, which are absent in the **PM 1** spectrum, clearly evidences the covalent binding of the dendron to NPs through an ester formation following the synthetic pathway 1.

NCD-2

Synthetic pathway 2 consisted in two steps: first the silane agent, APS, is coupled to the hydroxyl groups on the NPs' surface leaving amino groups exposed for further functionalizations. These reactive amines are then used in the second

ID: thangaraj.n Time: 20:51 I Path: N:/3b2/POLA/Vol00000/140260/APPFile/JW-POLA140260

J_ID: z8g Customer A_ID: POLA27375 Cadmus Art: POLA27375 Ed. Ref. No.: 14-0425.R1 Date: 28-August-14 Stage: Page: 6

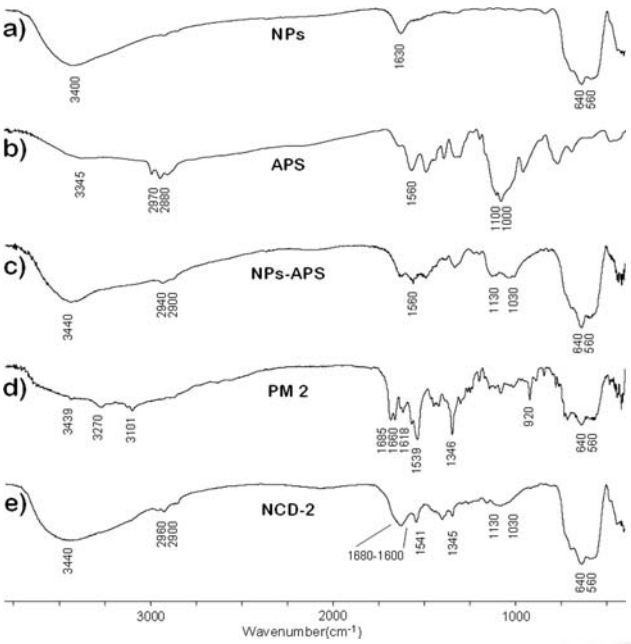

FIGURE 2 DRIFT spectra of the unmodified NPs (a); pure APS (b); NPs-APS (c); **PM 2**, the physical mixture between NPs-APS + **G1-NO$_2$** (d); and **NCD-2** (e).

synthetic step as linking points to anchor the dendron covalently through amide formation.

F2 Figure 2(a–e) shows the DRIFT spectra of the unmodified NPs, APS, amino silaned NPs (NPs-APS), a physical mixture formed by the freshly synthesized NPs-APS and the dendron (**PM 2**), and **NCD-2**.

Couplings of alcoxysilanes on oxide surfaces are proposed to occur through a multistep mechanism,[41–43] and their characterization is well documented. Based on this knowledge, Figure 2(c) shows the DRIFT spectrum of NPs-APS where all characteristic new signals associated with a successful silane coupling are present: aliphatic C-H coupling (2932 and 2876 cm^{-1}), N-H bending (1560 cm^{-1}), and Si-O-Si and Fe-O-Si asymmetric stretchings (1130–1030 cm^{-1}).

In the second step of pathway 2 the dendron was covalently attached to NPs-APS to obtain **NCD-2**. Note that the dendron could link to NPs-APS either by amidation through the exposed amino groups of the attached silane or by esterification through the hydroxyl moieties that remain on the NPs' surface. Although the higher nucleophilicity and mobility of the -NH$_2$ groups compared to the -OH moieties would favor the amidation pathway, it is important to consider that those amino groups could also be buried into silane layers and/or compromised in hydrogen bonding interactions, thus reducing their availability and accessibility towards any chemical functionalization.[44]

To further study the dendronized product **NCD-2**, a new control experiment was carried out similarly to the one performed before forming **PM 1**. To this end, a new physical mixture between NPs-APS and pure dendron was prepared (**PM 2**) and studied. Its DRIFT spectrum is shown in Figure 2(d). The frequency lowering of aromatic C-H stretching bands after dendronization was observed as for **PM1**, suggesting the successful covalent attachment of the dendron.

In relation to its precursor, NPs-APS, the DRIFT spectrum of **NCD-2** [Fig. 2(e)] shows new features: the broadening of the 2960–2900 cm^{-1} bands (C-H stretching), the broadening of the 1680–1600 cm^{-1} signal (sum of the Bands I-II of amide) and two new signals at 1541 and 1345 cm^{-1} (nitro asymmetric and symmetric stretchings, respectively). A decrease in the intensity of the 1130–1030 cm^{-1} signal (Si-O-Si and Fe-O-Si asymmetric stretchings) is also observed. After dendronization, such linkages are buried deeper into the organic layer and become less visible in the DRIFT spectra. Moreover, **NCD-2** spectrum also presents the broadening of the band located between 1680 and 1600 cm^{-1} (convolution of the bands I-II of the new amide groups), not observed in **PM 2**, thus also suggesting the successful covalent attachment of the dendron to NPs-APS.

Finally, it must be pointed out that while the reaction between the activated dendron, G1-ClNO$_2$, and the –OH from the NPs' surface is possible, no evidences of such esterification were ever found. Therefore, this reaction is assumed not to happen, or at least not in a significant manner.

NCD-3

Synthetic pathway 3 exploited the remaining hydroxyl groups from the γ-Fe_2O_3 on **NCD-1** after dendron binding as anchoring sites for the covalent coupling of APS as a synthetic complement. To the best of our knowledge, this kind of methodology is being presented for the first time ever in this article.

In relation to its precursors, **NCD-1** and APS [Fig. 3(a,b)], the spectrum of **NCD-3** [Fig. 3(c)] shows new features indicating the successful covalent attachment of APS: aliphatic C-H stretching signals evidenced as the broadening of the bands F3

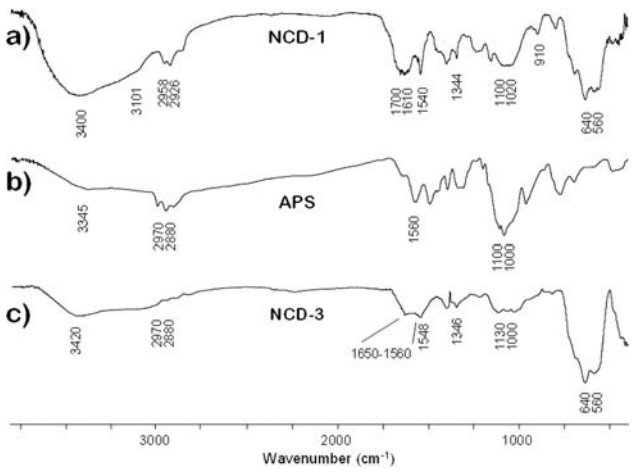

FIGURE 3 DRIFT spectra of **NCD-1** (a); pure APS (b); and **NCD-3** (c).

ID: thangaraj.n Time: 20:52 I Path: N:/3b2/POLA/Vol00000/140260/APPFile/JW-POLA140260

positioned at 2970 and 2880 cm^{-1}, N-H bending seen as the broadening of the 1650–1560 cm^{-1} band (overlapped with C=O ester stretching), and Si-O-Si and Fe-O-Si asymmetric stretchings confirmed as the broadening of the signals located between 1130 and 1000 cm^{-1} (overlapped with C-O ester stretching combination bands). It is worth mentioning that the signals corresponding to hydroxyl, amino, ester and nitro groups are present, albeit with a slight frequency variation in relation to the precursors; probably due to the formation of hydrogen bonding interactions among these moieties in the organic coating.[39]

TGA and TEM Characterization

F4 Figure 4 presents TGA studies carried out to gain better insights about the organic loading of the NPs and the effectiveness of each synthetic step.

As mentioned, the organic content of all modified NPs was obtained by TGA based on reported methods.[30,45] Figure 4(a) shows the thermograms of the unmodified and all modified NPs. Unmodified NPs showed only a slight weight loss below 220 °C, which was attributed to water loss. Systems NPs-APS, **NCD-1**, **NCD-2** and **NCD-3** also presented a minor weight loss until 250 °C of about 1% each, which is attributed to water and EtOH loss, the latter being from possible condensation reactions of any probably remaining unreacted Si-OEt groups from incomplete condensation during silanization steps.[46] All modified hybrid NPs showed their main weight loss between 250 and 800 °C as a multistep process corresponding to a progressive thermal decomposition of the organic content occurring in several closely related but undistinguished stages, thus making assignation of fragments impossible. Beyond 800 °C all thermograms remained constant. Thus, the thermal decomposition of the organic content of each system was ascribed to take place in the mentioned range of temperatures. Therefore, the organic content of every system as well as the organic loading achieved in every synthetic step are calculated by taking into consideration the weight loss between 250 and 800 °C. Clearly, a higher weight loss corresponds to a higher organic loading. The results show that **NCD-3** presents the highest organic content (10%), followed by **NCD-2** (6%), **NCD-1** (5%), NPs-APS (4%), and finally the unmodified NPs (0%).

As the success of each reaction to modify the NPs strongly depends not only on the nature and amount of functional groups on the substrate and the stoichiometry ratio, but also on their accessibility and availability, it was important to quantify their efficiency. Based on the previous TGA results and according to the way in which the synthetic strategy was carried out, the organic loading in each step—dendronization and silanization distinguished in the TGA plot in Figure 4(a) by black and grey brackets, respectively—is also determinable. This is possible because some of the already synthesized and characterized systems were indeed used as starting materials for the following steps. Thus, the organic loading for every step in each system was estimated and is presented in Figure 4(b). Note that the dendronization step

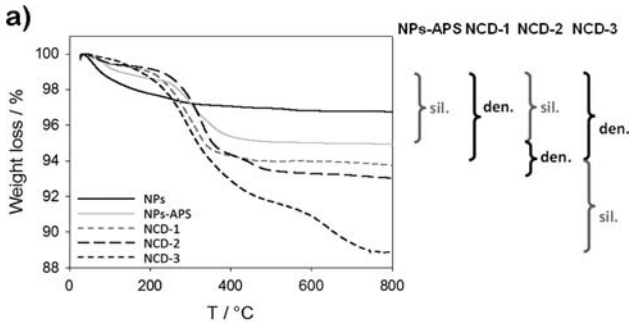

b)

NPs	NPs-APS	NCD-1	NCD-2	NCD-3	
-	4	-	4	5	silanization
-	-	5	2	5	dendronization
0	4	5	6	10	total organic loading (%)

FIGURE 4 (a) TGA thermograms of the unmodified and all modified NPs. The weight loss values of every synthetic step are indicated in black (dendronization) and grey (silanization) brackets, respectively. (b) Summary of the estimated organic contents achieved in every synthetic step for all systems.

on the unmodified NPs to generate **NCD-1** (5%) is more efficient than the one on NPs-APS to obtain **NCD-2** (2%). This indicates that the amine groups introduced as potential anchoring are less available than expected. This result is in agreement with the one previously reported by Panella et al.[47] showing that in APS-functionalized SiO_2-coated magnetic NPs the amount of amino groups chemically available to react via covalent binding is less than 40% compared to the value determined by TGA. Possible reasons for this reduced reactivity are that the incorporated amine groups on the NPs may be experiencing non-covalent interactions such as hydrogen bonding with -OH groups from the γ-Fe_2O_3, with other amines, and/or with remaining silanols, thus being less available for covalent binding.[44,48,49] Moreover, some amine groups may also be buried inside a three-dimensional polysiloxane layer resulting from a certain oligomerization of APS on the NPs' surface, being unreachable and therefore inaccessible to react.[49,50] Those situations combined (schematically represented in Scheme 2) produce S2
the lack of reactivity of the potential anchoring sites for the dendrons, making NPs-APS less reactive against dendronization than the unmodified NPs.

A different situation is observed for the silanization processes. APS functionalization of **NCD-1** to prepare **NCD-3** (5%) resulted slightly more efficient than the silanization of unmodified NPs to obtain NPs-APS (4%). This result may be explained in terms of the different dispersibility of the diverse substrates in the reaction solvent (toluene). **NCD-1** is much better dispersible in organic solvents than the unmodified NPs due to the compatibility between its organic content on the surface and the solvent, thus favoring not only

J_ID: z8g Customer A_ID: POLA27375 Cadmus Art: POLA27375 Ed. Ref. No.: 14-0425.R1 Date: 28-August-14 Stage: Page: 8

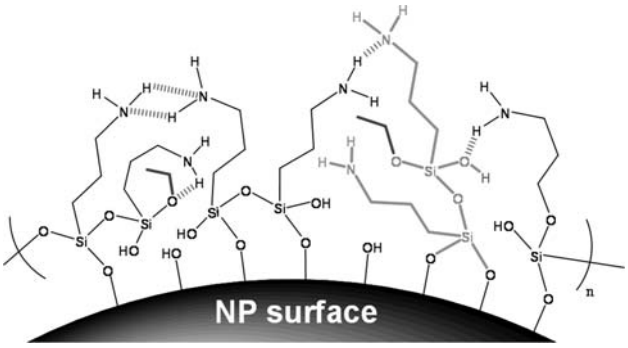

SCHEME 2 Simplified representation of non-covalent interactions and effects causing lack of reactivity on the introduced amine groups, such as H-bondings (||||||), oligomeric silane species responsible for burying amine groups (▬), and possible incomplete siloxane condensation reactions (▬). [Color figure can be viewed in the online issue, which is available at wileyonlinelibrary.com.]

AQ

the encounter between the different reactive species but also the reaction conditions.

TEM has also been exploited to study the surface modification of NPs demonstrating that a high silane grafting density onto magnetic NPs is observed in TEM images as a clear layer of different contrast covering the inorganic surface.[51] In our case, however, there is no noticeable contrasting halo surrounding the NPs for any of the modified NPs, as it can F5 be seen in Figure 5(a). This result is not only consistent with the idea of a low organic content, but also with the TGA results.

Finally, the low organic loading on the modified NPs and the nature of the modifiers preserve the magnetic character of the original NPs, as observed upon exposure to a magnet. Figure 4(b) shows that when the magnet is approached to the vessel the hybrid NPs go toward the magnet accumulating themselves against the wall, leaving a clear and translucent solution. The original perfectly dispersed system is easily reestablished after taking away the magnet and a short sonication time. It must be stated here that deeper studies of the magnetic properties of the modified NPs are beyond the scope of this work. Nevertheless, this feature could, eventually, be envisaged as a mean to purify systems where these NCDs are used as either nanomodifiers or functionalizable scaffolds, as previously reported for similar systems.[52]

UV-Vis Characterization. Study of Dispersibility and Stability of NP Dispersions

Stability of magnetic NP dispersions is a crucial requirement for almost any application.[43,53] While for biomedical applications water-dispersible iron oxide NPs are mostly used,[54,55] some other industrial and/or catalytic applications require magnetic NPs to be well dispersible in organic media.[56,57]

The dispersibility of the modified NPs was studied in different organic solvents. To this end, dispersions of identical concentration (0.005 mg mL^{-1}) were sonicated and the presence of nondispersed solid was evaluated qualitatively. The dispersibility order in DMSO is the following: **NCD-2** > **NCD-3** ≈ **NCD-1** >> NPs-APS ≈ NPs. Similar results were observed in DMAc and ACN. It must be noted that once dispersed, both unmodified NPs and NPs-APS precipitated very quickly, whereas all NCD dispersions did it at variable times.

As a way to quantify the different stabilities for the NCD systems, their spectral evolution as a function of time was studied and the absorbance decays were calculated after 12 min using the absorbance values at $\lambda = 400$ nm and using the following formula: Abs. decay = 100 ($Abs_{t=0\ min} - Abs_{t=12\ min}$)/ $Abs_{t=0\ min}$ (Fig. 6). To this end, solutions of APS and den- F6
dron [Fig. 6(a)], as well as dispersions of the unmodified and all modified NPs [Fig. 6(b)] were prepared and characterized by UV-vis spectroscopy using ACN as solvent. The spectrum of APS does not present any band in the studied range, while the dendron's spectrum presents a pronounced absorbance band at 237 nm (λ_{max}) and a shoulder located at 325 nm. Neither the unmodified NPs nor NPs-APS show any absorbance bands and only indicate the scattering of light and a noticeable spectral noise, likewise in the case of functionalized magnetite microspheres reported by Leung et al.[58] In contrast, the spectra of dendronized NPs (all three NCD systems) are similar to the spectrum of the free dendron since the mentioned absorbance bands are seen, although they appear remarkably blue-shifted to $\lambda_{max} \leq 230$ nm. **NCD-1** presents the lowest shifting ($\lambda_{max} = 230$ nm) whereas

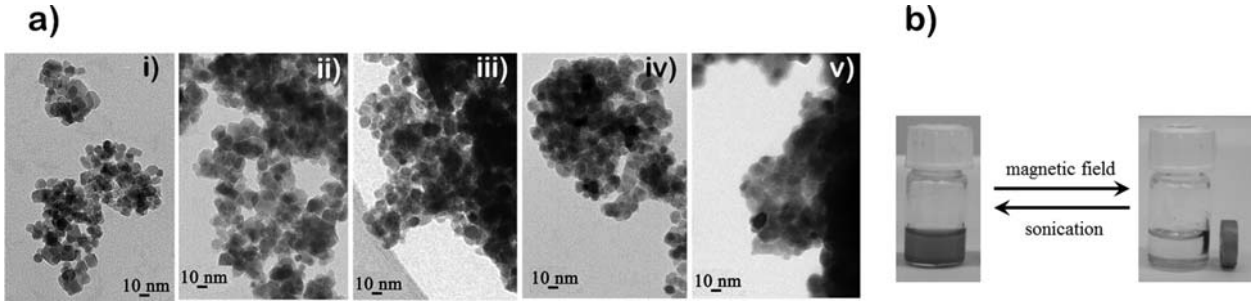

FIGURE 5 (a) TEM images of unmodified NPs (i), NPs-APS (ii), **NCD-1** (iii), **NCD-2** (iv), and **NCD-3** (v). (b) Photographs exhibiting the reversible behavior of the synthesized hybrid NPs before and after being exposed to a magnetic field, **NCD-2** is shown to exemplify the effect. [Color figure can be viewed in the online issue, which is available at wileyonlinelibrary.com.]

ID: thangaraj.n Time: 20:52 I Path: N:/3b2/POLA/Vol00000/140260/APPFile/JW-POLA140260

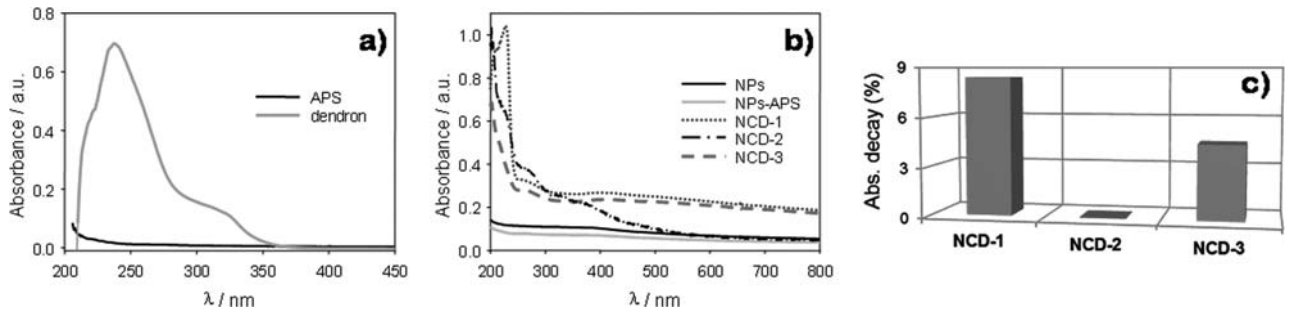

FIGURE 6 UV-Vis spectra of APS and dendron solutions in ACN (a). UV-Vis spectra of unmodified and modified NPs dispersions in ACN (b). Plot representing the absorbance decay (Abs. decay) determined for the NCDs dispersions(c). Abs. decay was calculated as follow: Abs. decay = 100 ($Abs_{t=0\ min} - Abs_{t=12\ min}$)/$Abs_{t=0\ min}$; where all absorbances were measured at 400 nm. Conditions: NCDs dispersions were 0.005 mg mL^{-1} in ACN and at 25 °C. [Color figure can be viewed in the online issue, which is available at wileyonlinelibrary.com.]

the λ_{max} of **NCD-2** and **NCD-3** are out of the measured UV window (i.e., $\lambda_{max} < 200$ nm). The blue-shifting in the absorbance bands of NCDs in relation to the free dendron spectrum accounts for an increase of the required energy for those electronic transitions to occur[59] when the dendron forms the organic layer. This effect could be originated in non-covalent interactions between adsorbate neighboring molecules among the organic layer (lateral interactions), for example through hydrogen bonding or aromatic π-stacking. Indeed, previous studies on the non-covalent adsorption of a pyrene derivative on carbon nanotubes via π-stacking interactions have evidenced a similar blue-shift.[60]

Considering that the lowest absorbance decay corresponds to the highest dispersion stability, the established order for the stability of all dispersions is as follow: **NCD-2** > **NCD-3** > **NCD-1** >>> NPs-APS ≈ NPs.

The combined results between the dispersibility and stability studies suggest that independently of the total amount of organic loading for each system, the solvation capability of their components is what favors both the dispersibility and the stability of the systems. It can be seen that the biggest effect is associated not only with the absence or presence of the dendron, but also with the way it is attached onto the NPs' surface. Thus, the highest dispersability and stability is achieved for the system where dendrons are attached to the particle surface through a flexible linker or spacer (**NCD-2**) enabling a much better solvation of the dendritic moiety, which then helps to stabilize the entire system. This effect is comparable to the steric stabilization of microgels due to the solubilization of the dangling chains on their surfaces.[35] Unlike **NCD-2**, **NCD-1,** and **NCD-3** bear exactly the same amount of dendrons covalently attached directly to the NPs' surface. These two systems presented similar dispersibilities, being in-between the most dispersible one (**NCD-2**) and the least dispersible ones (NPs-APS and unmodified NPs). However, their stabilities were very different. This difference is clearly caused by the APS contained in **NCD-3**, which is not present in **NCD-1**. Once again, we attribute this better stability of **NCD-3** compared to **NCD-1** to the better solvation of the organic modifiers on the particle surface. While the dendron moiety is similar in both systems, an extra contribution from the APS solvation may be the reason for an enhanced stability of **NCD-3** compared to **NCD-1**. Therefore, APS also influences the behavior of the NCDs, although in a less relevant manner than the dendron. Finally, the two systems where no dendrons were incorporated (NPs and NPs-APS) showed to be the least dispersible and the least stables. This result highlights the importance of the molecular ordering and how the role played by the silane and the dendron may modify the physicochemical properties of these hybrid nanomaterials. It must also be mentioned that **NCD-3**, which also shows good properties, presents the advantage of having, besides the dendrons and a silane layer, many fully functionalizable amine groups able to be exploited for different purposes toward a variety of applications.

Application of NCDs Toward the Generation of Electroactive GC Electrodes

The immobilization of NCDs on GC electrodes through self-assembly was carried out as schematically shown in Scheme 3. It has been demonstrated that the free dendron is capable to rapidly self-assemble on carbon surfaces through its aromatic moieties.[26,61] Thus, the presence of dendrons in the NCDs was exploited to act as a linker to efficiently immobilize the modified NPs onto carbon surface, while the nitro groups were expected to provide redox activity.[26,27] Scheme 3(a) shows that while all NCDs systems were successfully immobilized by self-assembly onto GC electrodes, the unmodified NPs and NPs-APS were not, even after subsequent prolonged immersion times. S3

Clearly, additional surface analyses are needed to know and understand the influence of the real organization and possible nanostructuration underwent by the NCDs on the GC surface. However, as they were electrochemically active, we focused this section on the feasibility of GC electrodes. Much emphasis was put on the electrochemical responses regarding the structural differences in each NCD studied. Thus, although the surface analysis would indeed provide

J_ID: z8g Customer A_ID: POLA27375 Cadmus Art: POLA27375 Ed. Ref. No.: 14-0425.R1 Date: 28-August-14 Stage: Page: 10

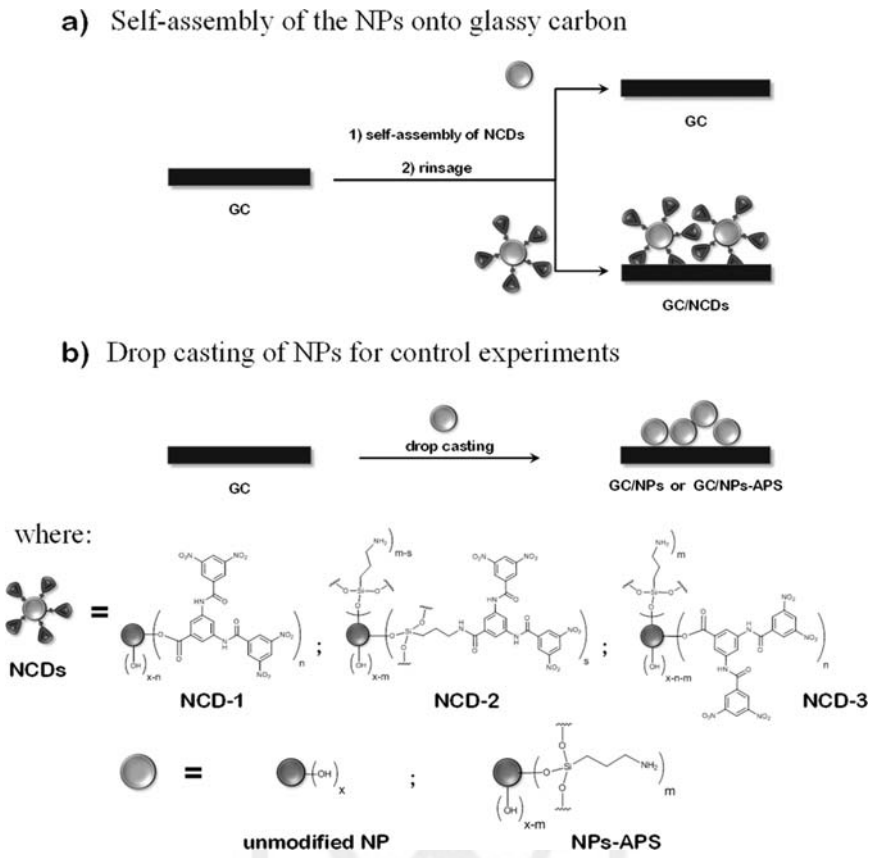

SCHEME 3 Schematic representation for the immobilization of all NPs onto GC surfaces following two different methodologies: self-assembly and drop casting. The successful self-assembly for all NCDs onto the GC surfaces could not be reproduced when unmodified NPs and NPs-APS were used instead (a). Therefore, a drop casting method had to be carried out to artificially immobilize the unmodified NPs and NPs-APS onto the GC surface (b). Conditions: 1 mg mL^{-1} dispersion of NCD in DMSO, $t = 15$ min to overnight. [Color figure can be viewed in the online issue, which is available at wileyonlinelibrary.com.]

important insights about the system as a whole, it was considered at this stage out of the scope on this particular publication.

The modified GC electrodes (GC/NCDs) generated by successfully attaching the NCDs onto GC surfaces were studied by cyclic voltammetry through the measurement of the electrochemical response of the nitro groups (Fig. 7).

To verify that all electrochemical responses were indeed generated by the nitro groups introduced on the GC electrodes by immobilization of the NCDs, the following control experiments were carried out. As unmodified NPs and NPs-APS could not be immobilized by self-assembly, they were deposited on the GC electrodes by drop-casting without any cleaning or purification step afterward [Scheme 3(b)]. The treated surface was then electrochemically characterized by cyclic voltammetry. The voltammograms of these two particular samples display only one cathodic peak at -0.30 V *vs.* Ag/AgCl, attributed to the irreversible reduction of the Fe^{3+} specie present in γ-Fe_2O_3 [see Fig. 7(a)]. This result is in agreement with those from the literature.[62] Thus, the lack of any other faradaic processes within the measured potential window indicates that no other electrochemically active group is present on the systems. This also suggests that all electrochemical responses observed for the GC/NCDs were indeed generated by the nitro groups belonging to the NCDs and that the presence of the Fe^{3+} species from NP core does not interfere with the visualization of the nitro response.

The voltammogram for the system GC/NCD-2 is shown as a model system in Figure 7(b), and the associated chemical transformation of the functional groups are shown in Figure 7(d). The cathodic waves at -0.48 V and -0.60 V during the first scan are associated to the four-electron reduction of each nitro moiety to the corresponding aryl hydroxylamine onto GC. On the subsequent sweep, the two pairs of anodic and cathodic peaks are attributed to the two-electron oxidation/reduction of the aryl-hydroxylamine/aryl-nitroso moieties. This behavior has been explained considering the differences in energy for the reduction of the two -NO_2 substituents in each aromatic ring of the dendron.[26]

The electrochemical responses observed for GC/NCD-1, GC/NCD-2, and GC/NCD-3 are qualitatively very similar, however it can be seen in Figure 7(c) that there are important quantitative differences in the measured charge density, according to the following order: **NCD-2 > NCD-3 > NCD-1**. This result

ID: thangaraj.n Time: 20:52 I Path: N:/3b2/POLA/Vol00000/140260/APPFile/JW-POLA140260

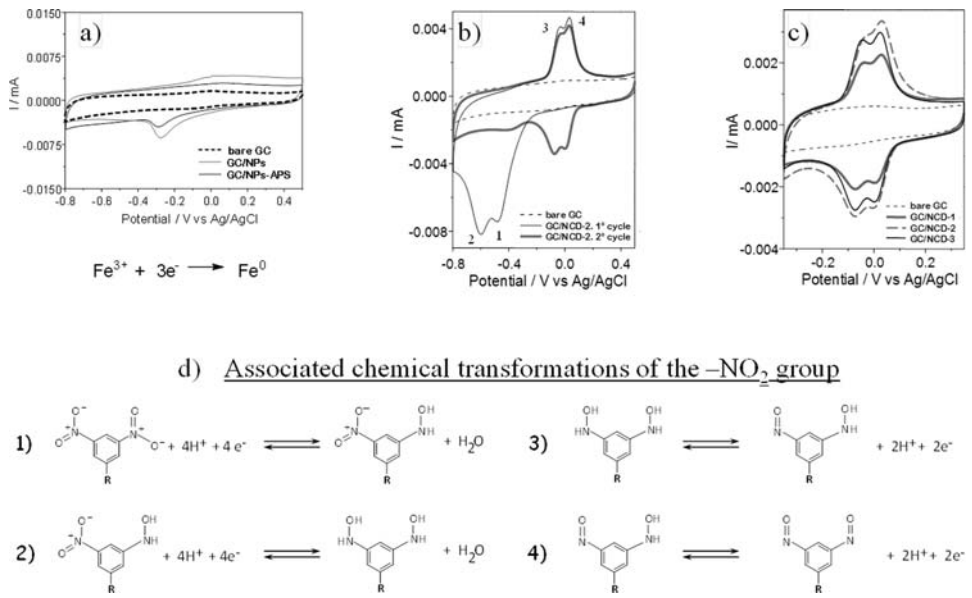

FIGURE 7 Cyclic voltamperommetric response measured for: a) bare GC, GC/NPs and GC/NPs-APS; b) **GCE/NCD-2** (first and second cycle); and, c) quantitative comparison between systems **GCE/NCD-1**, **GCE/NCD-2**, and **GCE/NCD-3**. The response of the bare electrode is also shown as reference. The associated chemical transformations of $-NO_2$ groups are shown for clarity (d). [Color figure can be viewed in the online issue, which is available at wileyonlinelibrary.com.]

evidences once again that the absence or presence of APS and also the role played by the APS and the dendron in the NCDs are of great significance toward the GC/NCD redox behavior, and thus the electrochemical response can be used to monitor this issue.

A comparison between **NCD-1** and **NCD-3** (both having the same dendron loading attached to the NPs' surface in the same way) reveals a higher value of charge related to nitro moieties for the APS-containing **NCD-3** than for **NCD-1**. This could probably be due to an enhanced stability and flexibility of the organic layer in the organic solvent caused by the complementary APS, what may improve the immobilization on GC. However, once again, **NCD-2** on GC gave the largest amount of attached nitro-groups, albeit it contains fewer dendrons than **NCD-3** and **NCD-1**. This result remarks the importance on the role of the dendron and the silane in the organic layer. When APS is used as a spacer the electrochemical response is better than when is used as a synthetic complement, which in turn is still better than when is not used at all. As a spacer, APS provides a short flexible segment between the rigid dendron and the hard NPs' surface that leads to a system with the highest dispersibility and stability. This fact seems to improve as well the efficiency of the self-assembly of **NCD-2** onto the GC surfaces, still maintaining the nitro groups available for further exploitation towards redox-active surfaces, which gave the best electrochemical response, as evidenced in Figure 7(c).

CONCLUSIONS

A combination of organic functionalizations consisting in silanization and dendronization was carried out on inorganic nanoparticles to synthesize three different redox-active hybrid NPs which can be considered as nanoparticle-cored dendrimers (NCDs). While silanization was performed to introduce architectural differences in the organic content, dendronization was carried out to introduce a high amount of electroactive $-NO_2$ groups.

The order in which the synthetic steps were carried out in each synthetic pathway to obtain the different NCDs affected the yields of the organic loading. Thus, dendronization gave an organic loading of 2% when performed after silanization, whereas direct dendronization onto the NPs' surface yielded 5%. However, the dendronization step seemed not to affect significantly the yield for the silanization process.

The chemical composition and the manner in which the organic layer was organized was also a consequence of the order in which the chemical modification were realized. These differences resulted in NCDs presenting different behaviors. Thus, the dispersibility order in DMSO, DMAc and ACN was: **NCD-2** > **NCD-3** ≈ **NCD-1** >> NPs-APS ≈ NPs, while the stability order was: **NCD-2** > **NCD-3** > **NCD-1** >>> NPs-APS ≈ NPs. **NCD-2** presented the best features. This can be understood by the good solubility of the dendron in the mentioned solvents and by the fact that in **NCD-2** the dendron moieties are more easily solvated than in any other system because of the flexible APS segment used as linker.

All hybrid NPs systems were used to generate redox-active GC electrodes. The differences in the final behavior of the electrodes were indeed due to the chemical structure and ordering of the beforehand synthesized NCDs. Only the dendronized NPs resulted electro-active, and although

J_ID: z8g Customer A_ID: POLA27375 Cadmus Art: POLA27375 Ed. Ref. No.: 14-0425.R1 Date: 28-August-14 Stage: Page: 12

qualitatively very similar, there were important quantitative differences (**NCD-2** > **NCD-3** > **NCD-1**) in their measured charge density.

It is worth noticing that contrary to the general idea where the silane coupling agent APS is used only to increase the reactivity of the –OH on NPs' surfaces, our results reveal the importance played by this agent to greatly enhance the overall properties of the formed NCDs as well as the electrodes fashioned by using those same hybrid NPs.

The combination of the results as a whole shown here put in evidence the relationship between physicochemical properties and chemical composition of the NCDs as well as the GC electrodes generated when using those NCDs as nanomodifiers. Finally, we expect both systems the NCDs themselves and the generated GC electrodes to be exploited in analytical and bio-sensing applications.

ACKNOWLEDGMENTS

This work has been founded by CONICET, ANPCyT, and SECYT of Universidad Nacional de Córdoba. J.I. Paez thanks CONICET for the fellowship provided. We also thank Lic. Melina Angelelli for her valuable contribution.

REFERENCES AND NOTES

1 M. Shen, X. Shi, *Nanoscale* **2010**, *2*, 1596–1610.

2 H. Liu, Y. H. Xu, S. H. Wen, Q. Chen, L. F. Zheng, M. W. Shen, J. L. Zhao, G. X. Zhang, X. Y. Shi, *Chem. Eur. J.* **2013**, *19*, 6409–6416.

3 V. Fischer, I. Lieberwirth, G. Jakob, K. Landfester, R. Munoz-Espi, *Adv. Funct. Mater.* **2013**, *23*, 451–466.

4 Y. Park, R. C. Advincula, *Chem. Mater.* **2011**, *23*, 4273–4294.

5 A. I. Lopez-Lorente, B. M. Simonet, M. Valcarcel, *Anal. Bioanal. Chem.* **2011**, *399*, 43–54.

6 S. H. Wen, F. Y. Zheng, M. W. Shen, X. Y. Shi, *Colloids Surf. A* **2013**, *419*, 80–86.

7 S. T. Selvan, T. T. Y. Tan, D. K. Yi, N. R. Jana, *Langmuir* **2010**, *26*, 11631–11641.

8 P. Froimowicz, R. Munoz-Espi, K. Landfester, A. Musyanovych, D. Crespy, *Curr. Org. Chem.* **2013**, *17*, 900–912.

9 P. Froimowicz, *Curr. Org. Chem.* **2013**, *17*, 891–891.

10 X. Hu, L. Zhou, C. Gao, *Colloid Polym. Sci.* **2011**, *289*, 1299–1320.

11 A. S. Goldmann, L. Barner, M. Kaupp, A. P. Vogt, C. Barner-Kowollik, *Prog. Polym. Sci.* **2012**, *37*, 975–984.

12 R. Sauer, P. Froimowicz, K. Schoeller, J.-M. Cramer, S. Ritz, V. Mailaender, *K. Landfester. Chem. Eur. J.* **2012**, *18*, 5201–5212.

13 C. Cardenas-Daw, A. Kroeger, W. Schaertl, P. Froimowicz, K. Landfester, *Macromol. Chem. Phys.* **2012**, *213*, 144–156.

14 P. Froimowicz, H. Frey, K. Landfester, *Macromol. Rapid Commun.* **2011**, *32*, 468–473.

15 M. Alvarez-Paino, G. Marcelo, A. Munoz-Bonilla, J. Rodriguez-Hernandez, M. Fernandez-Garcia, *Polym. Chem.* **2013**, *4*, 986–995.

16 Y.-S. Shon, In Advanced Nanomaterials; K. E. Geckeler, H. Nishide, Eds.; Wiley-VCH Verlag GmbH & Co. KGaA: Weinheim, Germany, **2010**; pp 743–766.

17 K. R. Gopidas, J. K. Whitesell, M. A. Fox, *J. Am. Chem. Soc.* **2003**, *125*, 6491.

18 J. I. Paez, M. Martinelli, V. Brunetti, M. C. Strumia, *Polymers* **2012**, *4*, 355–395.

19 Y. A. Wang, J. J. Li, H. Chen, X. Peng, *J. Am. Chem. Soc.* **2002**, *124*, 2293.

20 R. Wang, J. Yang, Z. Zheng, M. D. Carducci, J. Jiao, S. Seraphin, *Angew. Chem. Int. Ed.* **2001**, *40*, 549–552.

21 J. I. Paez, V. Brunetti, E. A. Coronado, M. C. Strumia, *Curr. Org. Chem.* **2013**, *17*, 943–955.

22 T. Joon Cho, R. A. Zangmeister, R. I. MacCuspie, A. K. Patri, V. A. Hackley, *Chem. Mater.* **2011**, *23*, 2665–2676.

23 J. I. Paez, E. A. Coronado, M. C. Strumia, *J. Colloid Interface Sci.* **2012**, *384* 10–21.

24 D. Choi, L. Chinn, Y. S. Shon, *Polym. Mater. Sci. Eng.* **2005**, *93*, 739–740.

25 E. C. Cutler, E. Lundin, B. D. Garabato, D. Choi, Y. S. Shon, *Mater. Res. Bull.* **2007**, *42*, 1178.

26 J. I. Paez, M. C. Strumia, M. C. G. Passeggi Jr., J. Ferrón, A. M. Baruzzi, V. Brunetti, *Electrochim. Acta* **2009**, *54*, 4192–4197.

27 J. I. Paez, P. Froimowicz, A. M. Baruzzi, M. C. Strumia, V. Brunetti, *Electrochem. Commun.* **2008**, *10*, 541–545.

28 P. Froimowicz, J. Paez, A. Gandini, N. Belgacem, M. Strumia, *Macromol. Symp.* **2006**, *245*, 51–60.

29 Y. Ishida, M. Jikei, M. A. Kakimoto, *Macromolecules* **2000**, *33*, 3202–3211.

30 M. Abboud, M. Turner, E. Duguet, M. Fontanille, *J. Mater. Chem.* **1997**, *7*, 1527–1532.

31 E. Marutani, S. Yamamoto, T. Ninjbadgar, Y. Tsujii, T. Fukuda, M. Takano, *Polymer* **2004**, *45*, 2231–2235.

32 I. García, N. E. Zafeiropoulos, A. Janke, A. Tercjak, A. Eceiza, M. Stamm, I. Mondragón, *J. Polym. Sci. Part A: Polym. Chem.* **2007**, *45*, 925–932.

33 The activation of the -COOH group of the dendron to form the acid chloride derivative was necessary since unactivated G1-NO2 proved ineffective to stabilize bare NP dispersions.

34 J. I. Paez, A. L. Cappelletti, A. M. Baruzzi, V. Brunetti, M. C. Strumia, *Macromol. Symp.* **2010**, *290*, 37–45.

35 P. Froimowicz, D. Klinger, K. Landfester, *Chem. Eur. J.* **2011**, *17*, 12465–12475.

36 P. J. Endres, T. Paunesku, S. Vogt, T. J. Meade, G. E. Woloschak, *J. Am. Chem. Soc.* **2007**, *129*, 15760–15761.

37 M. Joselevich, F. J. Williams, *Langmuir* **2008**, *24*, 11711–11717.

38 L. A. Porter Jr, D. Ji, S. L. Westcott, M. Graupe, R. S. Czernuszewicz, N. J. Halas, T. R. Lee, *Langmuir* **1998**, *14*, 7378–7386.

39 R. Paulini, B. L. Frankamp, V. M. Rotello, *Langmuir* **2002**, *18*, 2368–2373.

40 N. Griffete, F. Herbst, J. Pinson, S. Ammar, C. Mangeney, *J. Am. Chem. Soc.* **2011**, *133*, 1646–1649.

41 N. Frickel, R. Messing, T. Gelbrich, A. M. Schmidt, *Langmuir* **2010**, *26*, 2839–2846.

42 R. M. Pasternack, S. R. Amy, Y. J. Chabal, *Langmuir* **2008**, *24*, 12963–12971.

43 S. Laurent, D. Forge, M. Port, A. Roch, C. Robic, L. Vander Elst, R. N. Muller, *Chem. Rev.* **2008**, *108*, 2064–2110.

44 P. Froimowicz, J. I. Paez, L. Gerbino, S. N. Ali, N. Belgacem, A. Gandini, M. Strumia, *Macromol. Res.* **2012**, *20*, 800–809.

ID: thangaraj.n Time: 20:52 I Path: N:/3b2/POLA/Vol00000/140260/APPFile/JW-POLA140260

45 A. Noomane, S. Hbaieb, M. -A. Bolzinger, S. Briançon, Y. Chevalier, R. Kalfat, *Colloids Surf. A* **2014**, *441*, 653–663.

46 H. H. Hinterwirth, M. Strobl, H. Al-Dubai, *Monatshefte Fur Chem.* **2010**, *141*, 291–299.

47 B. Panella, A. Vargas, D. Ferri, A. Baiker, *Chem. Mater.* **2009**, *21*, 4316–4322.

48 A. Rodriguez-Cano, P. Cintas, M.-C. Fernandez-Calderon, M.-A. Pacha-Olivenza, L. Crespo, L. Saldana, N. Vilaboa, M. -L. Gonzalez-Martin, R. Babiano, *Colloids Surf. B* **2013**, *106*, 248–257.

49 Y. Liu, Y. Li, X.-M. Li, T. He, *Langmuir* **2013**, *29*, 15275–15282.

AQ2

50 U.S. Patent US00,770,454,3B2, **2010**.

51 X. Zheng, S. Luo, L. Zhang, J. -P. Cheng, *Green Chem.* **2009**, *11*, 455–458.

52 D. H. K. Reddy, S. -M. Lee, *Adv. Colloid Interface Sci.* **2013**, *201*, 68–93.

53 A. -H. Lu, E. L. Salabas, F. Schüth, *Angew. Chem. Int. Ed.* **2007**, *46*, 1222–1244.

54 L. H. Reddy, J. L. Arias, J. Nicolas, P. Couvreur, *Chem. Rev.* **2012**, *112*, 5818–5878.

55 N. A. Frey, S. Peng, K. Cheng, S. Sun, *Chem. Soc. Rev.* **2009**, *38*, 2532–2542.

56 C. L. Augustyn, T. D. Allston, R. K. Hailstone, K. J. Reed, *RSC Adv.* **2014**, *4*, 5228–5235.

57 C. W. Lim, I. S. Lee, *Nano Today* **2010**, *5*, 412–434.

58 K. C. Leung, S. Xuan, C. M. Lo, *ACS Appl. Mater. Interfaces* **2009**, *1*, 2005–2012.

59 D. A. Skoog, F. J. Holler, T. A. Nieman, Principles of Instrumental Analysis; McGraw Hill, **2001**.

AQ3

60 V. Georgakilas, V. Tzitzios, D. Gournis, D. Petridis, *Chem. Mater.* **2005**, *17*, 1613–1617.

61 E. D. Farías, V. Brunetti, J. I. Paez, M. C. Strumia, M. C. G. Passeggi, J. Ferrón, *Microsc. Microanal.* **2014**, *20*, 61–65.

62 L. H. M. Fonseca, A. W. Rinaldi, A. F. Rubira, L. F. Cótica, S. N. d. Medeiros, A. Paesano Jr, I. A. Santos, E. M. Girotto, *Mater. Chem. Phys.* **2006**, *97*, 252–255.

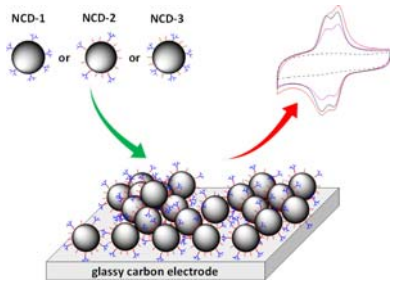

Nanoparticle-cored dendrimers (NCDs) with diverse chemical and structural features are synthesized via surface functionalization of iron oxide nanoparticles and by combining a silane coupling agent and dendritic moieties. The nanostructure of the material is controlled not only by the information programmed into the dendritic branches, but also by the presence of other organic molecules within the modifying layer, by the molecular ordering, and by the interaction between the different modifiers and with the dispersing media, affecting macroscopic and physicochemical properties.

AQ1: Please provide at least three keywords from the common keyword catalog located at http://onlinelibrary.wiley.com/journal/10.1002/(ISSN)1099-0518/homepage/Keywords.pdf.

AQ2: Kindly provide the author name and company name for the Ref. 50.

AQ3: Kindly provide the publisher location details for the Ref. 59.

AQ4: Please confirm whether the color figures should be reproduced in color or black and white in the print version. If the color figures must be reproduced in color in the print version, please fill the color charge form immediately and return to Production Editor. Or else, the color figures for your article will appear in color in the online version only.